Monitoring saltwater corrosion of steel using ultrasonic coda wave interferometry with temperature control

Maxime Farin, Emmanuel Moulin, Lynda Chehami, Farouk Benmeddour, Cyril Nicard, Pierre Campistron, Olivier Bréhault, Lucie Dupont

Ultrasonics 124 (2022) 106753

Contents lists available at ScienceDirect

Ultrasonics

journal homepage: www.elsevier.com/locate/ultras

Monitoring saltwater corrosion of steel using ultrasonic coda wave interferometry with temperature control

Maxime Farin [a,*], Emmanuel Moulin [a,b], Lynda Chehami [a], Farouk Benmeddour [a,b], Cyril Nicard [c], Pierre Campistron [a], Olivier Bréhault [a], Lucie Dupont [a]

[a] Univ. Polytechnique Hauts-de-France (UPHF), Univ. Lille, CNRS, Centrale Lille, UMR 8520 - IEMN - Institut d'Electronique, de Microélectronique et de Nanotechnologie, F-59000 Lille, France
[b] INSA Hauts-de-France Le Mont Houy, F-59313 Valenciennes, France
[c] Univ.Lille, CNRS, INRAE, Centrale Lille, UMR 8207, UMET, Unité Matériaux et Transformations, 59000 Lille, France

ARTICLE INFO

Keywords:
Coda wave interferometry
Corrosion
Non destructive testing

ABSTRACT

Assessing corrosion is crucial in the petrochemical and marine industries. Usual ultrasonic methods based on pulse-echo and guided waves to detect corrosion lack of precision and struggle in structures with a complex shape. In this paper, a complementary and sensitive ultrasonic method based on coda wave interferometry is presented to detect and quantify thickness loss caused by saltwater corrosion of a steel sample. The method consists in exciting the sample and measuring periodically the scattered coda signal. Correlation of the coda signal with a reference taken for the sample initial state permits the monitoring of corrosion spread with a high accuracy. A laboratory experiment is conducted with two steel samples immersed in saltwater with coda and temperature measured simultaneously. One of the samples is protected from corrosion and is used as a control sample to determine the influence of temperature on the coda signals. It is shown that the coda signals on the corroded sample can be temperature-corrected using the temperature measurement only. A control sample is not needed. A good correlation is found between a parameter quantifying the stretching of the coda over time and the corrosion surface, which is monitored with a camera. Finally, a simple theoretical model of coda signal is proposed to quantify the real-time average corrosion rate during the experiment with a sub-micrometric precision. The estimated final average corrosion depth is validated by independent depth profile measurements. The uncertainties and sensitivity of the presented method are investigated.

1. Introduction

Corrosion can significantly reduce the lifetime of metallic structures and cause their failure. Efficiently monitoring the rate of corrosion is a major safety, financial and environmental issue in the petrochemical and marine industries. Numerous complementary Non Destructive Testing (NDT) methods exist to quantify the corrosion [e.g. with ultrasound, electromagnetic or optical fiber sensors, see Refs. 1,2, for review]. The corrosion chemical reaction can be directly measured, with e.g. electrochemical sensors, but most of the NDT methods are indirect and monitor the mass or thickness loss of the investigated metallic structure. The simplest method consists in having a coupon composed of the same material and in the same corrosive conditions as the tested structure and to regularly retrieve this sample to measure its mass. However, this method is unpractical and does not permit a real time monitoring of the corrosion rate.

Ultrasonic approaches are popular because they are relatively cheap, can be used remotely and are able to detect corrosion beneath a protection coating without needing the sensor to be embedded in the structure. There are two main ultrasonic approaches to measure corrosion in the literature. The first one, pulse-echo, consists in sending a pulse with a piezoelectric sensor and measure its echoes off the opposite walls of the tested sample [3–6]. The time between the arrivals of the two echoes is proportional to the sample thickness and decreases as corrosion progresses because the average thickness decreases (Fig. 1a). Interestingly, Zou and Cegla [5] showed that ultrasonic signals do not capture the loose corrosion deposits that accumulate at the surface but are only sensitive to the thickness loss. The second main ultrasonic approach (pitch-catch) consists in exciting selected guided waves which are sensitive to surface roughness and record how these eigenmodes are modified because of the scattering, reflections or mode conversions caused by surface corrosion [7–11]. Guided wave techniques are usually more sensitive than pulse-echo to track changes in wall thickness and are particularly useful to inspect large areas

* Corresponding author.
E-mail address: maxime.farin@uphf.fr (M. Farin).

https://doi.org/10.1016/j.ultras.2022.106753
Received 9 November 2021; Received in revised form 20 March 2022; Accepted 21 April 2022
Available online 27 April 2022

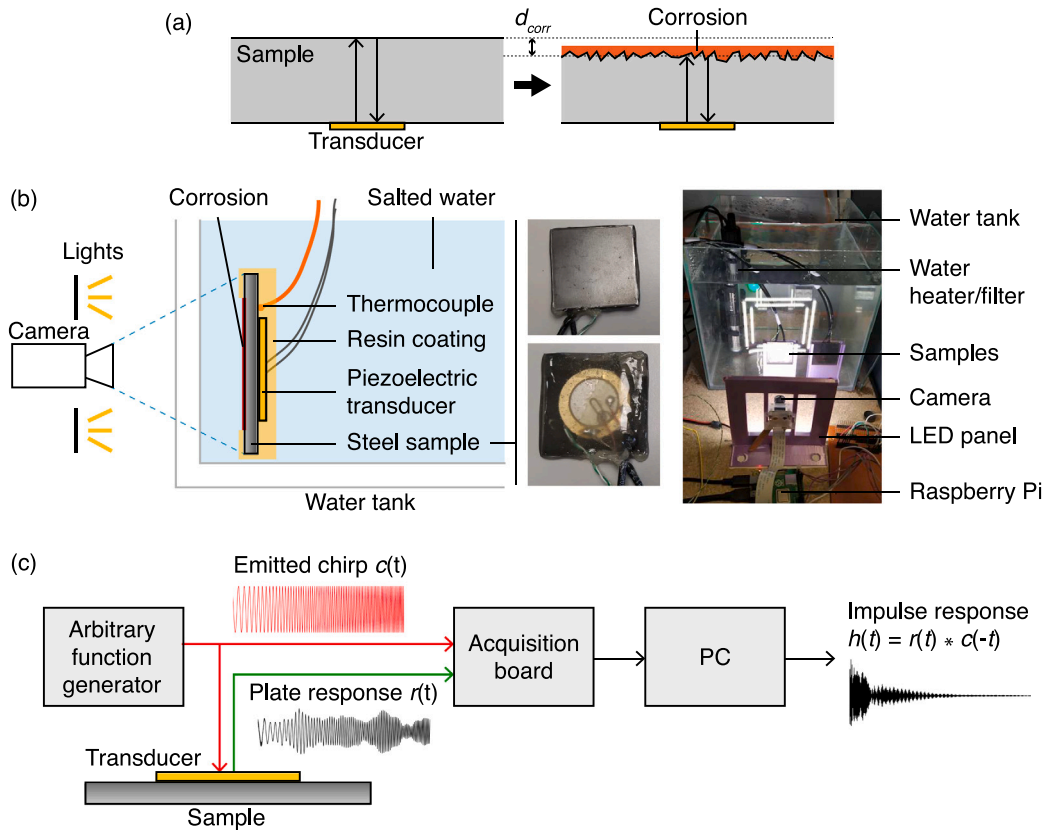

Fig. 1. (a) Schematic of the principle of the acoustic methods to detect the average thickness loss caused by corrosion. (b) Schematic and picture of the experimental setup. (c) Schematic of the process to record coda signals.

which are difficult to access with other NDT methods. In addition to these two main ultrasonic approaches, some authors conducted passive corrosion monitoring by tracking the ultrasonic acoustic emissions caused by bubble break-up or rupture of the passive film at the surface of austenitic stainless steel samples but the acoustic emission amplitude is so low that this method is compromised by environmental noise in field applications [12,13]. Finally, Hogg et al. [14] applied nonlinear ultrasonic resonant spectroscopy to detect stress corrosion cracking on a stainless steel rod. They excited a resonance of the rod and observed that its amplitude and the shift in its frequency as the excitation amplitude increases is more important when the rod has been exposed for a longer time to a corrosive environment.

In this paper, an alternative and complementary ultrasonic corrosion monitoring method based on coda wave interferometry (CWI) is presented. CWI was initially introduced by Snieder at al. [15] as a seismic method to evaluate local variations in wave velocities in the ground. When a structure is excited with a pulse and its response is measured, the coda signal consists of the waves reflected multiple times off the structure boundaries and heterogeneities. This signal is very reproducible as long as no changes occur in the elastic properties or geometry of the tested structure. However, if any heterogeneity appears, such as corrosion roughness, small delays are introduced on the wave paths and will accumulate over the multiple reflections. As a result, the coda signal is sensitive to damage that would remain undetectable by first arrival waves. The principle of CWI is to compare e.g., with correlation, the state of the coda at a given time with that of a reference coda signal measured for the structure initial state. CWI is often used to track local wave velocity, stress and temperature anisotropies or water front progression in the ground or in concrete [16,17] [see 18, for review]. Chen et al. [19] showed that CWI can track the real time cleaning of a biofilm (wax layer) at the surface of a stainless steel plate. In their experiment, a piezoelectric emitter/receiver transducer is glued to the plate, on the face opposite to the wax layer. At different times, the transducer excites the structure with an ultrasonic pulse and measures the coda signal scattered in the plate and the wax layer. As the wax layer is cleaned over time with a hot water flow, the correlation coefficient of the coda signal with respect to its initial shape decreases and stabilizes when the wax layer is completely cleaned off. The authors also detected fouling formation using the same technique [20]. In the present paper, the same approach as Chen et al. [19] is applied to track the thickness thinning of a steel sample in saltwater. To the authors' best knowledge, CWI has never been used to monitor corrosion. The diffuse coda is potentially more sensitive to changes in wall thickness than the pulse-echo and pitch-catch techniques, which are based on the first arrival waves that interact only once with the corroded surface during their propagation. Moreover, CWI performs well in structures with a small size, a complex shape or an heterogeneous composition, i.e. where guided waves methods struggle, because more reflections imply a longer coda signal. More importantly, since it is based on comparison with a reference, CWI does not rely on the *a priori* knowledge of the corroding structure geometry.

It is worth noting that the coda signal is not only sensitive to the apparition of damage but is also extremely sensitive to any environmental changes that affect wave velocities in the structure such as temperature variations [21]. Therefore, it is important to measure these environmental parameters or work in conditions where they do not change to be able to track changes caused by corrosion only. In this paper, high frequencies (between 5 MHz to 15 MHz) are investigated to excite longitudinal waves reflecting off the opposite faces of a steel plate-like sample (Fig. 1a). Doing so, the measured coda is not sensitive to boundary conditions along the sides of the sample, but only to thickness loss caused by corrosion and to the temperature.

The objective of this research work is to show that observed changes in the coda signal measured on a corroding steel sample can be used

as a real-time and precise indicator of the corrosion onset and spreading. The experimental setup is described in Section 2. In Section 3.1, the parameters to quantify the evolution of the coda signal during a corrosion experiment are presented and the influence of temperature on the coda signal is determined. Then, a corrosion experiment is conducted in saltwater with simultaneous coda and temperature measurements. The evolution of the coda signal is compared with the corrosion surface measured using a camera. Finally, in Section 4.1, a simple theoretical model of coda signal is presented to interpret the experimental results and quantify the time-varying corrosion rate during the experiment. The estimated final corroded depth is compared with depth measurements conducted after the corrosion experiment.

2. Experimental setup

The paper is devoted to observe how the coda signal measured on a steel sample is related to the average thickness loss caused by corrosion over time. To do so, an emitter/receiver piezoelectric transducer (of diameter 2 cm) is glued onto a 4-by-4 cm^2, 2 mm thick steel plate (Fig. 1b). In order to protect the transducer from saltwater, the sample surface with the transducer is casted into epoxy resin. A thermocouple is also casted into epoxy resin beside the transducer to measure the sample temperature. The exposed face of the sample, opposite to the transducer, is ground with fine sandpaper to make it more vulnerable to corrosion. In order to correct the measured coda signal from the temperature bias, a second sample is prepared. This 'control sample' is cut from the same plate and has same dimensions as the first sample ('test sample') but its exposed surface is protected from corrosion with an anti-corrosion varnish. The idea is to use the coda signal variations caused by temperature on the control sample to compensate those variations on the test sample and therefore observe the influence of corrosion only on the coda signal of the test sample. This method was introduced by Zhang et al. [17] to correct the coda signal measured on a concrete pillar subjected to a tensile test from the temperature bias. Temperature compensation of the coda signal is detailed in the next section.

The two prepared samples are set vertically on a 3D-printed stand inside a water tank (Fig. 1b). The mechanical stresses applied on the samples do not vary during the experiments so that the measured coda signal is only affected by corrosion and temperature. A camera regularly takes pictures of the exposed surface of the test sample. Temperature measurement and picture capture are performed with a Raspberry Pi 4B board and python programming language. A LED panel ensures a constant lighting of the sample throughout the experiment. The tank and the LED panel are installed in an opaque box so that the captured pictures are not affected by daily light changes. The tank is filled with saltwater with 3% NaCl. Constant temperature (±1 °C) and water cleanness are maintained using a heater set at 30 °C and a water pump and filter. A high water temperature implies a higher corrosion rate than can be observed in the sea and thus allow to reduce the duration of the experiment.

The coda is the part of the sample impulse response $h(t)$ after the first wave arrivals. To measure $h(t)$, a frequency-modulated (chirp) signal $c(t)$ of duration 1 ms with frequency varying linearly with time from 5 MHz to 15 MHz is generated by an arbitrary waveform generator (*DG4162*, Rigol) and excites the piezoelectric transducer. The induced vibration response $r(t)$ of the sample is recorded by the receiver with an acquisition board (14-bit, *PicoScope 5444D*, Pico Technology) at sampling frequency 125 MS s^{-1}. The sample response is $r(t) = h(t) * c(t)$ where $*$ is the convolution product (Fig. 1c). Finally, the impulse response $h(t)$ of the sample is retrieved by convoluting the measured response by the conjugate of the emitted chirp: $r(t) * c(-t) = h(t) * c(t) * c(-t) \simeq h(t)$, assuming that the chirp autocorrelation $c(t) * c(-t)$ approximates to the delta distribution $\delta(t)$ (Fig. 2a). $h(t)$ is averaged over 20 measurements to minimize background noise in the coda signal, without any amplification of the excitation signal needed.

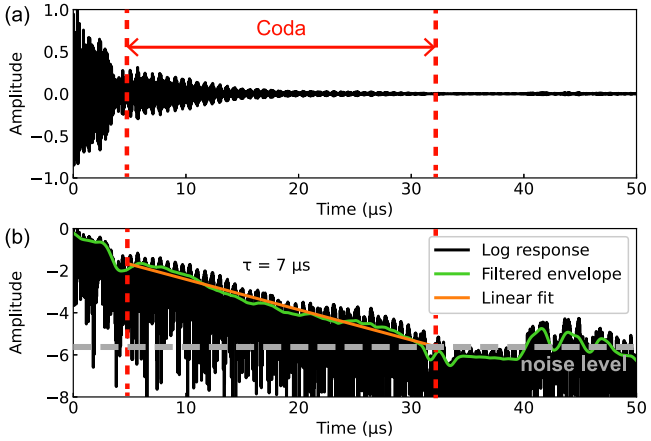

Fig. 2. (a) Impulse response measured on a steel sample immersed in saltwater. (b) Logarithm impulse response.

Signal emission, acquisition and processing are performed using python and the *picosdk* library to communicate with the PicoScope. In the following, t_{exp} refers to the time of acquisition of the coda signal and temperature and t refers to the time within a coda signal.

The frequency range of excitation from 5 MHz to 15 MHz was chosen to excite longitudinal waves propagating in the sample thickness and reflecting multiple times off the sample opposite faces. These waves are not very sensitive to side boundary conditions but are sensitive to the changes occurring in front of the piezoelectric transducer such as variations of the sample thickness caused by corrosion. The amplitude of a diffuse coda typically decays with time t as $\exp(-t/\tau)$ with τ, the characteristic attenuation duration (Fig. 2b). In the tested steel samples immersed in saltwater, the coda is observed between $t \simeq 5$ μs and $t \simeq 30$ μs. Before $t \simeq 5$ μs, the wave field is not diffuse yet and after $t \simeq 30$ μs, the background noise level is reached. In the following, 'early coda' refers to the coda signal when the signal amplitude starts to decay exponentially and 'late coda' refers to the signal just before reaching noise level. The attenuation time τ is estimated to be about 7 μs by fitting a linear law to the logarithm envelope amplitude. The characteristic attenuation time τ is about 10 times longer than the approximate time-of-flight duration of waves reflected off the sample opposite faces $\Delta t = \frac{2e}{v_L} \simeq 0.66$ μs, with $e = 2$ mm, the thickness and $v_L \simeq 6020$ m s^{-1}, the longitudinal wave velocity. Considering that noise level is reached after about $t \simeq 4\tau$, the variations in the sample thickness have been probed about 40 times in the late coda.

3. Experimental results

3.1. Quantification of the coda signal variation

A way to quantify how much the coda evolves over time due to corrosion or temperature is to measure the correlation coefficient between a section of the coda at a given time t_{exp} since the start of the experiment and the same coda section at a reference time $t_{exp} = 0$ corresponding to the sample initial state. Practically, the decorrelation of coda sections $s_1(t)$ and $s_2(t)$ in the time window $t \in [t_1, t_2]$ i.e., $D = 1 - C$, with C, the correlation coefficient, is

$$D = 1 - \frac{s_1(t)s_2(t)}{\sqrt{\int_{t_1}^{t_2} s_1(t)^2 \mathrm{d}t \int_{t_1}^{t_2} s_2(t)^2 \mathrm{d}t}}. \quad (1)$$

The decorrelation coefficient D varies between $D = 0$, corresponding to identical signals, and $D = 2$, corresponding to signals with opposite phases. A decorrelation $D = 1$ means that the signals are completely uncorrelated ($C = 0$). The duration of the correlation windows is arbitrarily chosen to be about ten periods of waves at the average

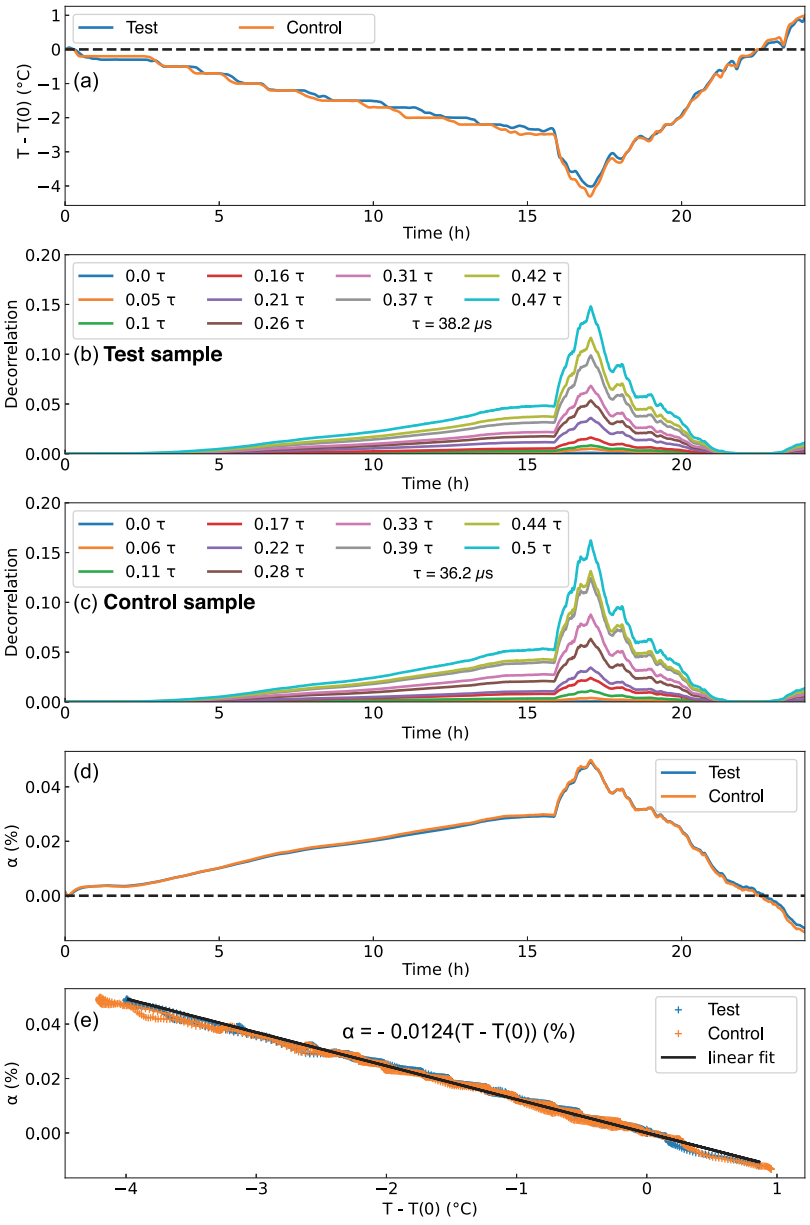

Fig. 3. (a) Variation of temperature T with respect to its value at the start of the experiment $T(t_{exp} = 0)$ for two 4-by-4 cm^2, 2 mm thick steel plates in air during 24 h. (b) and (c) Decorrelation curves of the (b) test and (c) control samples for different starting times of the correlation window, normalized by the characteristic attenuation time $\tau \simeq 37$ μs (different colors). The correlation window duration is 1 μs. (d) Coda stretching factor α of the two samples. (e) Coda stretching factor α as a function of the temperature variation $T - T(t_{exp} = 0)$. A linear fit is given (full line).

frequency of the coda signal i.e. here $t_2 - t_1 \simeq 1$ μs. The late coda signals are more sensitive to damage apparition but they are also more sensitive to the noise level. Decorrelation windows can typically be observed before $t \sim 4\tau \simeq 25$ μs, after which the signal-to-noise ratio is too low and the decorrelation coefficient D rapidly diverges, independently of corrosion.

Coda variations over time can also be quantified using a single parameter representing the stretching of the coda signal. Assuming constant velocity variations and a homogeneous media, the time shift (positive or negative) between the measured and reference codas increases linearly with time t in the coda [21]. Consequently, the waveform after the perturbation appears stretched with respect to the reference waveform $h_0(t)$ as $h_0(t(1+\alpha))$ with α, a real coefficient that quantifies the coda stretching with respect to the reference coda, and also represents the relative change in wave velocity in the sample $\alpha = \Delta v/v_0$ [17]. Temperature can also cause the sample to dilate when temperature increases but Rommetveit et al. [3] showed that changes on wave velocities caused by temperature affects ultrasonic signals significantly more than sample dilatation. To estimate the factor α for a given measurement time t_{exp}, stretched signals $h_0(t(1+a))$ are computed using the reference coda signal $h_0(t)$ for a range of factors $a \in [-0.5, 0.5]$ %. Then, all $h_0(t(1+a))$ signals are correlated with the coda signal $h(t)$ measured at time t_{exp}. The maximum of correlation is for $a = \alpha$.

3.2. Influence of temperature on coda signal

As temperature increases, the wave velocity v decreases and the coda appears elongated with respect to a reference for a lower temperature [17,21,22]. In other words, the stretching factor $\alpha = \Delta v/v_0$ decreases. To correct the coda signals on the tested sample from the temperature bias, the procedure of Zhang et al. [17] is followed. At each measurement time t_{exp}, the coda stretching factors are measured on the tested and control samples (α_{test} and $\alpha_{control}$, respectively) and are

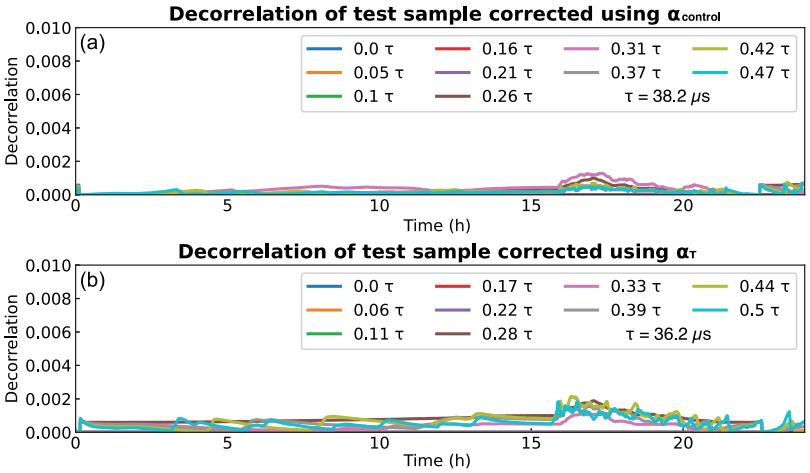

Fig. 4. (a) and (b) Decorrelation curves of the test sample in air obtained after de-stretching the coda signals using factor α deduced (a) from control sample coda signals and (b) from temperature $T - T(0)$, using the linear law found in Fig. 3e. The different colors represent different starting times of the 1 μs-long correlation window, normalized by the characteristic attenuation time $\tau \simeq 37$ μs.

differentiated to obtain the coda stretching factor $\alpha_{corr} = \alpha_{test} - \alpha_{control}$ corresponding to corrosion only.

First, the relation between α and the temperature is evaluated on the steel samples. To do so, the coda decorrelation is measured every two minutes on the two dry samples exposed to the room temperature for 24 hours (h). The results are presented in Fig. 3. During the experiment, temperature first decreases constantly, then decreases more sharply at $t_{exp} \simeq 16$ h and finally increases after $t_{exp} \simeq 17$ h (Fig. 3a). The decorrelation curves follow well the temperature on both samples, with the reference coda signal taken at $t_{exp} = 0$ (Fig. 3b and 3c). The decorrelation returns to 0 around $t_{exp} \simeq 23$ h when the temperature reaches its initial value. It is clear that the later coda time windows are more affected by temperature than the earlier ones. The coda stretching factor α quantifying how much the coda is stretched with respect to its reference at $t_{exp} = 0$ also shows a similar variation as the decorrelation curves (Fig. 3d). Note that α is very similar on both samples, which confirms that the temperature influence on the coda signal on the control sample is representative to that observed on the test sample. As expected, the coda stretching factor α is inversely proportional to the temperature variation $T - T(t_{exp} = 0)$ (Fig. 3e). The best fit to the data is $\alpha \simeq -0.0124(T - T(t_{exp} = 0))$ (in %). This law depends *a priori* only on the sample constituting material and not on its dimensions because α represents the wave velocity variation within the plate thickness in the investigated frequency range from 5 MHz to 15 MHz.

The factor $\alpha_{control}$ measured on the control sample can be used to correct the stretching caused by temperature variations on the test sample by 'de-stretching' each coda signal $h(t)$ at measurement time t_{exp} as $h(t/(1 + \alpha_{control}(t_{exp})))$. The decorrelation curves obtained from corrected coda signals on the test sample are shown in Fig. 4a. The decorrelation caused by the temperature variations is well compensated ($D < 0.002$). There is no residual decorrelation because the samples did not corrode and the influence on the coda of the other environmental parameters (e.g. pressure, humidity) is negligible. The coda signals on the test sample can also be de-stretched using the factor α_T deduced from the temperature variation (Fig. 4b). Consequently, a temperature measurement seems sufficient to correct decorrelation curves from temperature variations. This is confirmed in the following corrosion experiment.

3.3. Influence of saltwater corrosion on coda signal

A corrosion experiment is now conducted in saltwater as described in Section 2. The test sample can corrode but the control sample is protected from corrosion and is dedicated to show the coda stretching caused by temperature variations. Coda is measured every two minutes for 60 h and the reference coda is chosen at the moment when the samples are immersed. The results of this experiment are presented in Fig. 5. During the experiment, the temperature varies with a saw-like pattern caused by the fact that the water heater successively turns on and off to maintain water temperature around 30 °C (Fig. 5a). Note that the temperature was not measured between $t_{exp} = 5$ h and $t_{exp} = 6.5$ h due to a Raspberry Pi failure. The temperature variation is clearly visible in the decorrelation curves of both samples (compare Fig. 5a with 5b and 5c). On the test sample, the decorrelation D reaches almost 2 in the late coda ($t > 2\tau$) and then decreases (Fig. 5b). In contrast, on the control sample, all decorrelation curves stay lower than $D = 0.1$ for the whole experiment (Fig. 5c). The coda stretching factor α_{test} increases up to 0.4% on the corroded sample (Fig. 5d). On the control sample, $\alpha_{control}$ follows closely the one deduced from temperature variation (α_T) using the scaling law from Fig. 5e. The coda stretching factor α_{corr} caused by corrosion only can be deduced by subtracting the factor measured on the test sample with that measured on the control sample ($\alpha_{test} - \alpha_{control}$) or with that deduced from temperature ($\alpha_{test} - \alpha_T$). Both are close to each other and the temperature-related saw-like variations are not visible any more. This confirms that a control sample is not needed to correct the coda from temperature bias but only an independent temperature measurement. The fact that the stretching caused by corrosion increases during the experiment can be explained as follows. As the sample thickness decreases, the time-of-flight duration of waves in the thickness decreases. Consequently, wave fronts arrive slightly earlier at the transducer and the coda signal appears compressed with respect to its initial state reference, as if the wave velocity increased. Therefore, $\alpha = \frac{\Delta v}{v_0}$ increases.

Similarly as in Section 3.2, the decorrelation curves are corrected to remove the effect of temperature (Fig. 6). The corrected curves are similar for both methods of estimating the α due to temperature variations (with the control sample or with the temperature, Fig. 6a and 6b). By de-stretching each coda signal $h(t)$ at measurement time t_{exp} on the test sample as $h(t/(1+\alpha_{test}(t_{exp})))$ using factor the stretching factor α_{test} measured on the same sample, all the decorrelation caused by phase shifting can be removed (Fig. 6c). The residual decorrelation is caused by amplitude variations in the coda only but stays below $D = 0.1$ i.e., much lower than the decorrelation caused by coda stretching. One can therefore assume that the presence of corrosion mostly stretches the coda signal with respect to the initial state reference, at least at high frequencies.

The pictures of the exposed face of the sample throughout the experiment reveal that corrosion spreads rapidly after the start of the

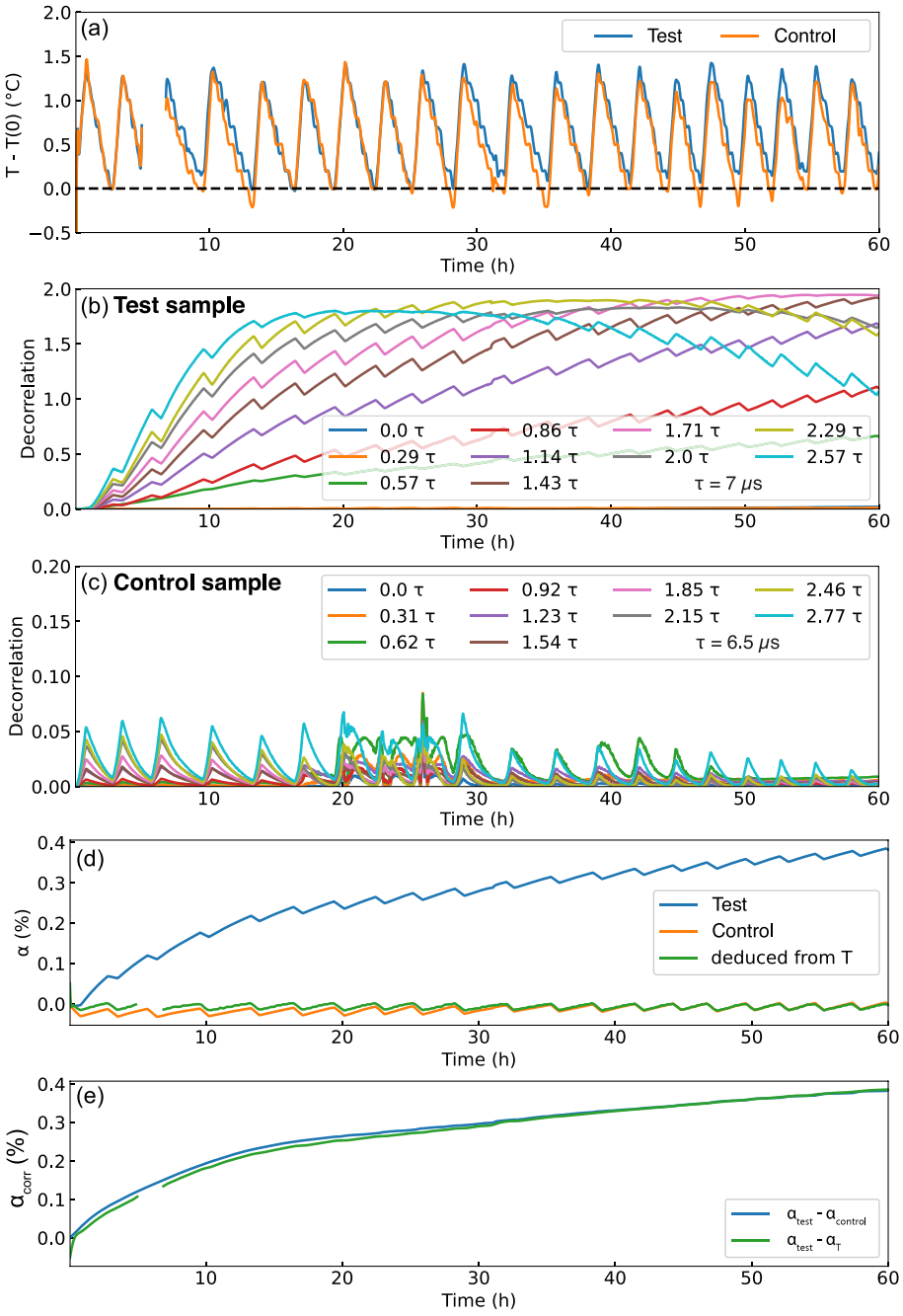

Fig. 5. Two 4-by-4 cm^2, 2 mm thick steel samples are immersed in saltwater during 60 h. (a) Temperature measured on each sample with respect to the temperature at the start of the experiment. (b) and (c) Decorrelation curves on the (b) test and (c) control samples for different starting times of the correlation window, normalized by the characteristic attenuation time $\tau \simeq 7$ μs (different colors). (d) Coda stretching factor α of the two samples and α_T deduced from temperature variation on the test sample, using the scaling law of Fig. 3e. (e) Coda stretching factor caused by corrosion α_{corr}.

experiment, with most of the final corroded surface reached before $t_{exp} = 5$ h (Fig. 7a). After $t_{exp} = 5$ h, the corroded surface does not grow much any more but the corrosion patch slightly changes of color. In order to verify whether the measured coda stretching (Fig. 7b) is representative of the corrosion spreading, it is compared with an independent parameter related to corrosion: the average pixel value of the pictures of the sample surface (Fig. 7c). Both the stretching factor α_{corr} and the average pixel value strongly increase at the start of the experiment, up to about $t_{exp} \simeq 15$ h and $t_{exp} \simeq 7$ h, respectively. After $t_{exp} \simeq 15$ h, the stretching factor continues to increase linearly with time until the end of the experiment while the average pixel value stabilizes and saturates to its final value after $t_{exp} \simeq 35$ h. An excellent correlation is observed between the coda stretching factor α_{corr} and the average pixel value until $t_{exp} \simeq 5$ h. Therefore, the parameter α_{corr} is a good indicator of corrosion onset. After $t_{exp} \simeq 7$ h, α_{corr} continues to increases while the pixel value stabilizes, possibly indicating that corrosion continues to occur below the apparent brown patch. In the next section, the average corrosion depth in the present experiment is quantified using a simple model.

4. Discussion

4.1. A simple model to quantify corrosion depth from coda signal

A simple theoretical model of synthetic coda signals in a sample of varying thickness is proposed in order to estimate the average corroded

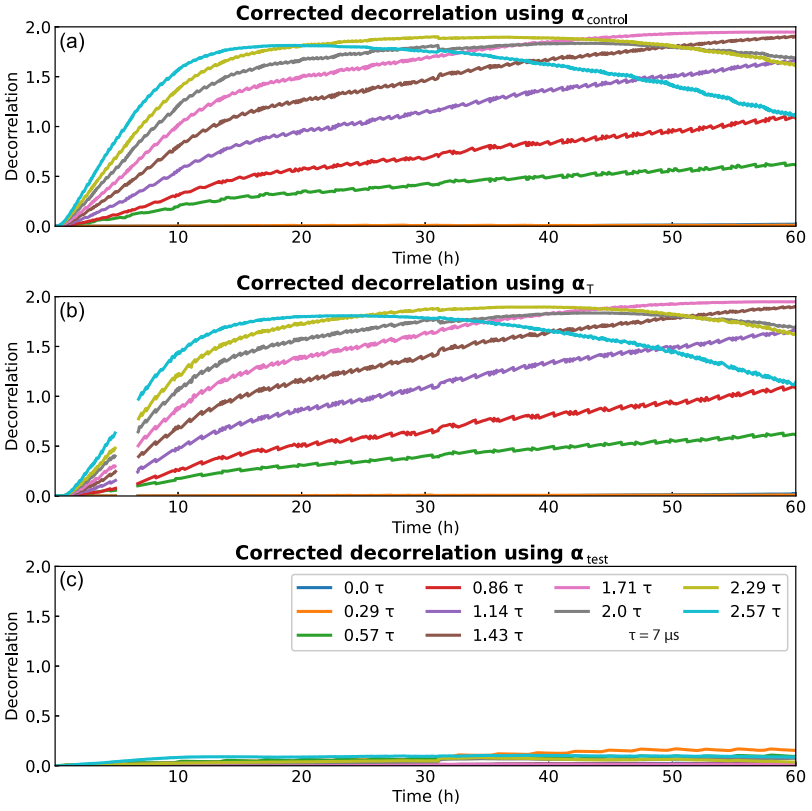

Fig. 6. (a) and (b) Decorrelation curves of the test sample in saltwater obtained after de-stretching the coda signals using factor α due to temperature deduced from (a) the control sample coda signal, (b) temperature variation (using the linear law found in Fig. 3e). (c) Decorrelation curves of the test sample obtained after complete de-stretching of the coda signals. The different colors represent different starting times of the 1 μs-long correlation window, normalized by the characteristic attenuation time $\tau \simeq 7$ μs.

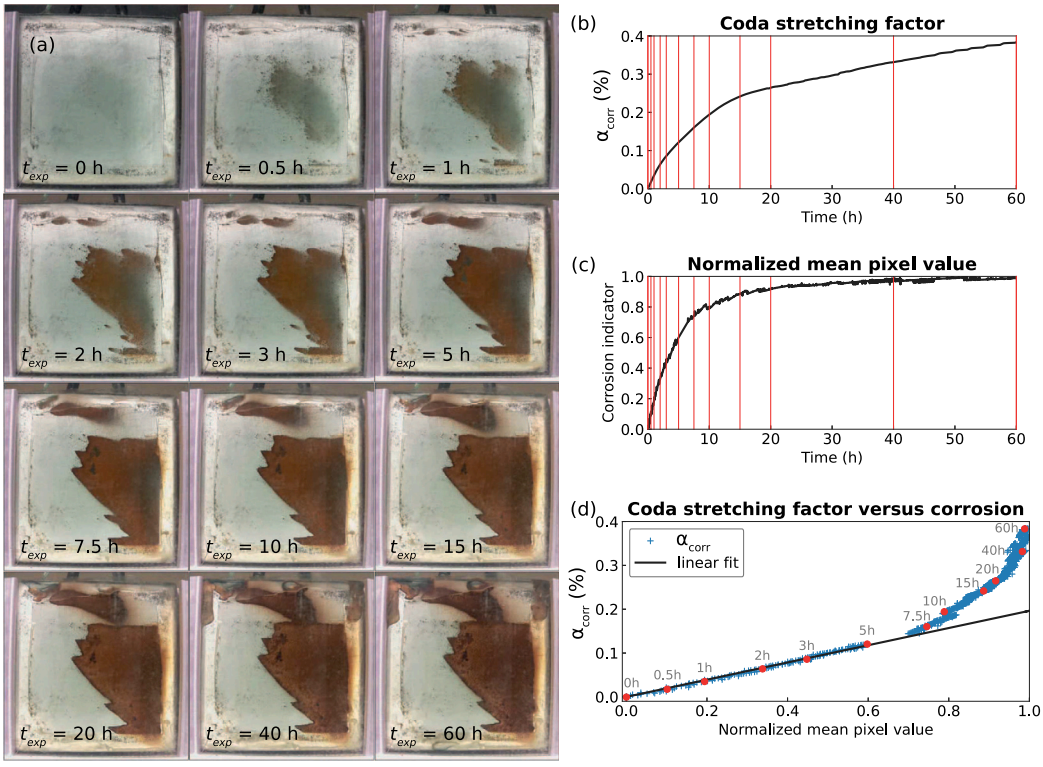

Fig. 7. (a) Pictures of the corrosion of the test sample during the 60 h experiment in saltwater. (b) Coda stretching factor caused by corrosion α_{corr} and (c) Normalized mean pixel value in the pictures of the experiment. (d) Coda stretching factor α_{corr} as a function of the normalized pixel value. The data of the first 5 h of the experiment are fitted with a linear law. The times of the pictures in (a) are indicated with vertical red lines in (b) and (c) and with red dots in (d).

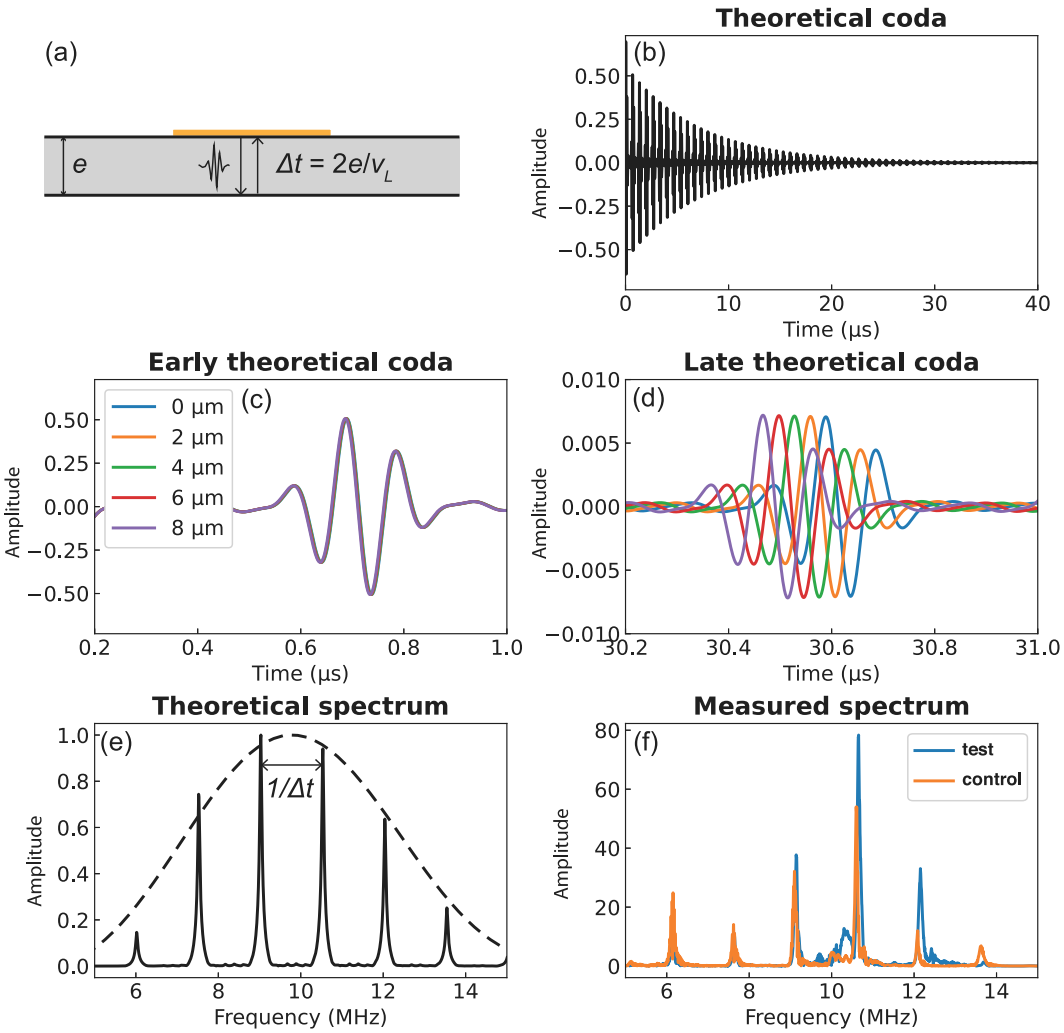

Fig. 8. (a) Schematic of the physical model to describe wave propagation at high frequencies in plates. (b) Theoretical coda signal obtained by summing impulses arriving at multiples of Δt. (c) Early and (d) Late coda signal in the physical model at 10 MHz for different average corrosion depths. (e) and (f) Normalized amplitude spectrum of (e) the intact plate in the 10 MHz physical model and (f) measured at the beginning of the 60 h corrosion experiment in saltwater for both samples. In panel (e), dashed lines show the normalized amplitude spectrum of one impulse.

depth from the experimental results. At 10 MHz, the wavelength of compressional waves is about $\lambda \simeq 0.6$ mm. In the experiment, the investigated samples are plate-like structures of thickness $e = 2$ mm $\simeq 3.3\lambda$. In this context, it is assumed that the recorded impulse response is composed of the multiple reflections of the original emitted pulse off the plate opposite faces, each reflection arriving at multiples of the time-of-flight duration $\Delta t = 2e/v_L$ (Fig. 8a). A synthetic coda signal is computed by summing pulses consisting of a period of a 10 MHz sine wave every multiples of Δt (Fig. 8b). The signal is multiplied by $\exp(-t/\tau)$, with $\tau = 7$ μs, the characteristic attenuation time measured during the experiment in saltwater, and filtered between 5 and 15 MHz, to reproduce the characteristics of the experimental signals. The amplitude spectrum of this signal is a comb of pulses separated by frequency $1/\Delta t \simeq 1.5$ MHz and modulated by the amplitude spectrum of a single 10 MHz sine period (Fig. 8e). A similar amplitude spectrum is observed in the laboratory experiment, when exciting the 2 mm thick samples in the frequency range from 5 MHz to 15 MHz (Fig. 8f). Synthetic coda signals are computed for different average corroded depths d_c, i.e. for thicknesses $e = 2mm - d_c$. The early coda is similar for all tested thicknesses (Fig. 8c). However, as the corrosion depth d_c increases, the time-of-flight duration Δt is slightly shorter and the time shifts accumulate over the multiple wave reflections, so that the pulses arrive slightly earlier in the late coda (Fig. 8d).

Similarly as in the laboratory experiments, the coda stretching factor α is computed for these synthetic coda signals. As expected, α is observed to be proportional to the average corrosion depth d_c (Fig. 9a). This linear scaling is used with the factor α_{corr} measured during the 60 h experiment in saltwater (Fig. 5e) to deduce the instantaneous average corrosion depth during the experiment (Fig. 9b). This curve is time-derivated to get the average corrosion rate (Fig. 9c). The corrosion rate is initially around 25 μm per day and rapidly decays to reach a constant rate of about 1 μm after $t = 20$ h. This evolution is in agreement with early corrosion rates of steel coupons in saltwater estimated by Melchers and Jeffrey [23] by periodically weighting the coupons. A chemical explanation of why the corrosion rate is initially high and then decays to finally stabilize is given by the authors. In the present experiment, the final average corrosion depth of the test sample is estimated to be about 8 μm. This depth is validated by surface scans of the test sample performed with a profilometer (*Alpha Step IQ*, SCIENTEC with 50 μm s^{-1} scan speed): the final corroded depth varies between 0 and 16 μm (±20 nm) and its average is very close to the depth of 8 μm estimated from α_{corr} (Fig. 10).

Finally, theoretical coda decorrelation curves are computed using the synthetic coda signals corresponding to the coda stretching factor α_{corr} measured during the experiment (Fig. 5e). The modeled decorrelation curves are quantitatively very close to the measured ones corrected from temperature variations, although slightly lower (Fig. 9d and 9e).

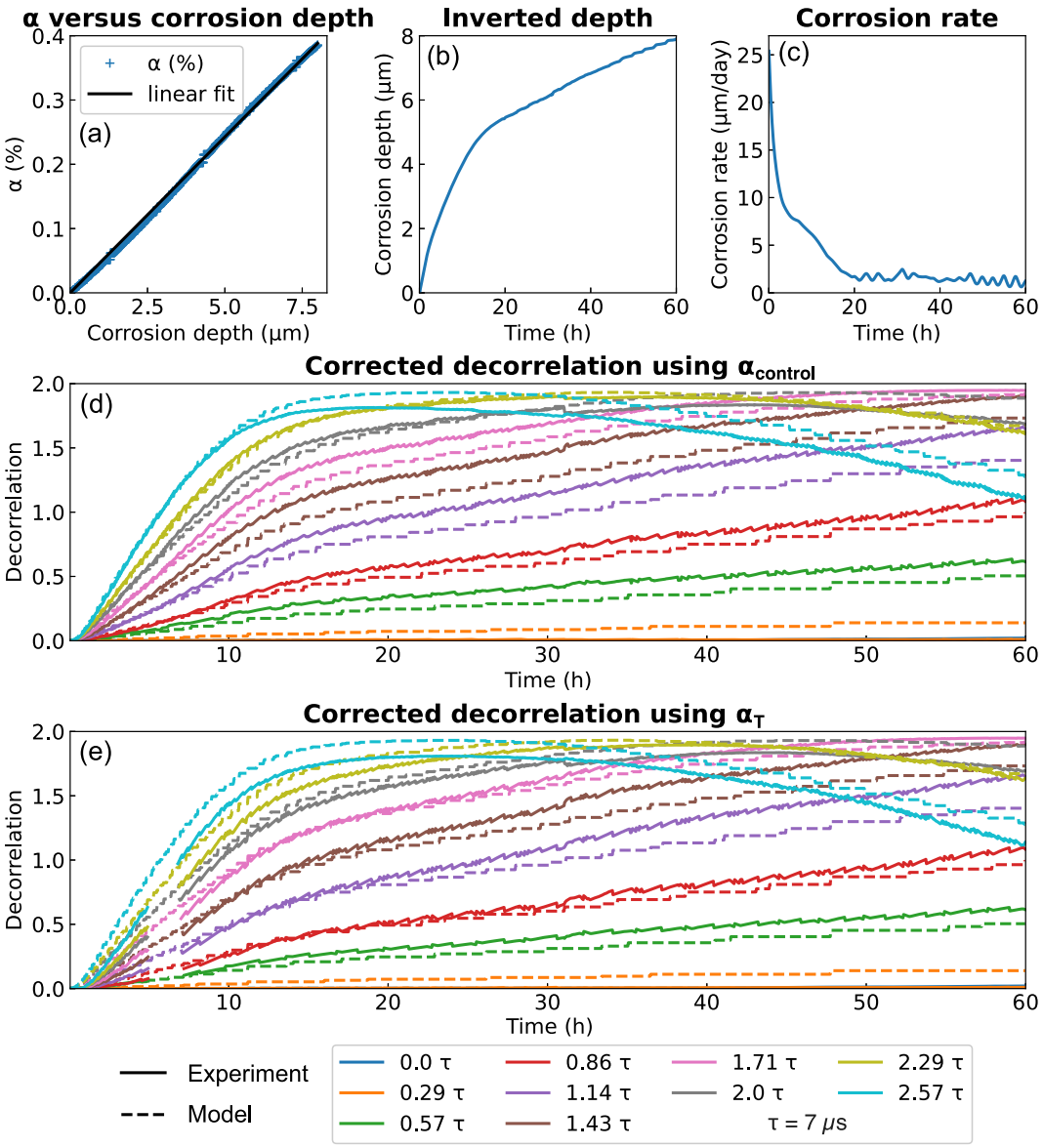

Fig. 9. (a) Coda stretching factor α of synthetic coda signals for different plate thicknesses (corrosion depths). (b) Average corrosion depth during the 60 h experiment in saltwater estimated using the coda stretching factor α_{corr} from Fig. 7b and the scaling low of panel (a). (c) Corrosion rate as a function of time. (d) and (e) Temperature-corrected decorrelation curves from Fig. 6ab (full lines) and decorrelation curves computed from synthetic coda signals (dashed lines). The different colors represent different starting times of the 1 μs-long correlation window, normalized by the characteristic attenuation time $\tau \simeq 7$ μs.

The slight discrepancy might come from the fact that the surface of the sample was partially corroded in the experiment, contrary as assumed in the model (Fig. 7a). Indeed, only the thickness of the sample intervenes in the model, which supposes that the sample is corroded uniformly over its whole surface. That said, the simple model of longitudinal waves reflected off the opposite sample faces seems to accurately describe the laboratory observations and quantifies the instantaneous sub-micrometric average corrosion depth from the coda stretching factor α_{corr}. The computation of the average corrosion depth could be implemented in real time during a corrosion experiment if both the coda stretching factor and the temperature are measured with the same apparatus.

4.2. Uncertainty on the corrosion depth estimate

The uncertainty on the corrosion depth estimated with the CWI method is evaluated. Some uncertainty arises from the determination of the coda stretching factor α. As described in Section 3.1, to estimate the value of α at a given time t_{exp}, the reference coda signal $h_0(t)$ is stretched as $h_0(t(1+a))$, for a range of factors a and the stretched signals $h_0(t(1+a))$ are then correlated with the coda signal $h(t)$ measured at time t_{exp}. The maximum of correlation corresponds to $a = \alpha$. Since the correlation coefficient as a function of a can be noisy, this function is fitted with a gaussian law and the maximum of the gaussian is chosen as the maximum of correlation. Sometimes, the maximum of the correlation coefficient and the maximum of the fitted gaussian may not exactly match, which implies a slight uncertainty on the value of α and therefore on the corrosion depth. The resulting precision on the corrosion depth is estimated to be about 0.07 μm. Another source of uncertainty on the corrosion depth comes from the computation of the stretching factor α_{corr} caused by corrosion by differentiating the stretching factor α_{test} measured on the test sample either with that measured on the control sample ($\alpha_{test} - \alpha_{control}$) or with that deduced from temperature ($\alpha_{test} - \alpha_T$) (Fig. 5). The precision on α_{corr} resulting from using one or the other approaches is in average about 0.005%, i.e. about 0.1 μm on the corrosion depth. Consequently, the total precision on the corrosion depth evaluated with the CWI method presented

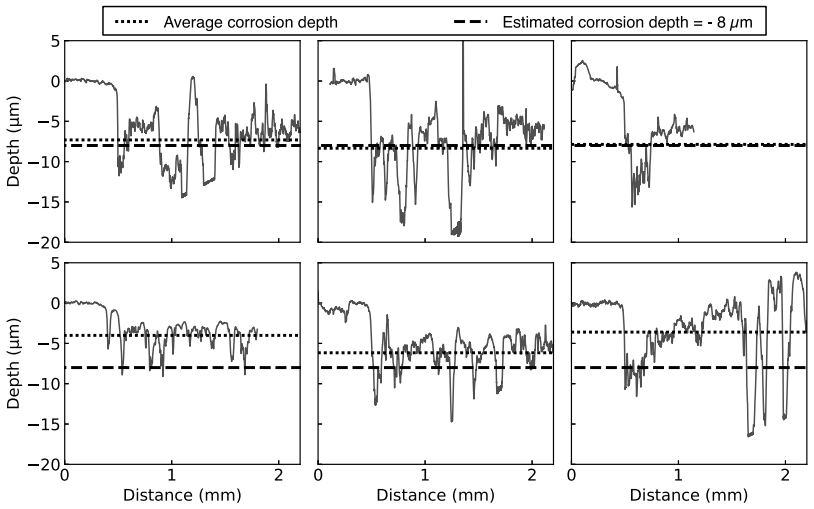

Fig. 10. Six profiles of depth scanned at the surface of the corroded sample at the end of the experiment in saltwater. Depth of 0 μm corresponds to the uncorroded part of the sample. The expected average depth of 8 μm is indicated by a dashed line and the measured average corroded depth is indicated by a dotted line.

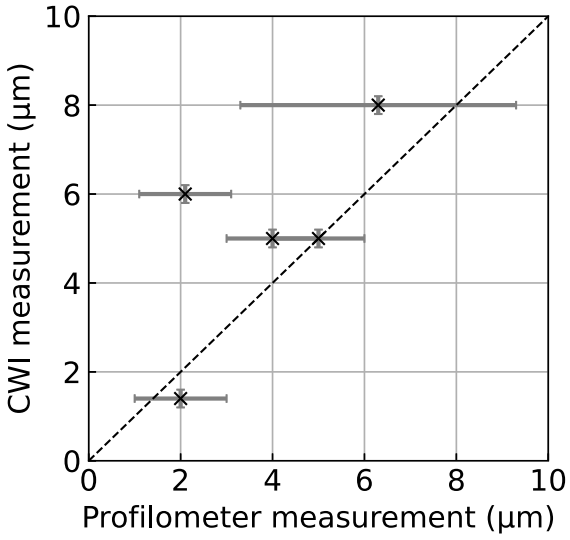

Fig. 11. Comparison of the final average corrosion depth measured with a profilometer with that estimated with the method presented in this paper for five corrosion experiments of 2 mm thick steel samples in salted water.

in this paper is approximately 0.2 μm. For the final corrosion depth of 8 μm obtained in the above experiment, the uncertainty is 2.5%.

4.3. Repeatability

To verify whether the method is robust, four additional corrosion experiments of 2 mm thick steel samples in salted water have been conducted and the final average corrosion depth estimated with CWI is compared with that measured with the profilometer (Fig. 11). A good agreement is observed. Note that the uncertainty of the profilometer measurement is high (more than ±1 μm) because the corrosion depth is heterogeneous and is estimated from a few millimeter long profiles (cf Fig. 10). In contrast, CWI gives an estimate of the sample corrosion depth averaged over the surface of the piezoelectric transducer.

4.4. Sensitivity range

One of the assumption of the coda model proposed in Section 4.1 is that the lateral dimensions of the sample do not affect the measurement of the corrosion depth because, at high frequency from 5 MHz to 15 MHz, the piezoelectric transducer is mainly sensitive to the reflections of longitudinal waves in the sample thickness. This assumption is verified with an experiment on a 10-by-4 cm^2, 2 mm thick steel plate with three piezoelectric transducers side-by-side (Fig. 12a). The plate is left in air for an hour and the decorrelation of the coda is measured on all three transducers (Figs. 12a-c). At $t_{exp} = 30$ min, a drop of water is deposited in front of one transducer (at position $x = 0$). The observed decorrelation D is respectively 10 and 20 times smaller for the transducers at $x = 2.7$ cm ($D < 0.02$) and $x = 5.4$ cm ($D < 0.01$) from the drop than for the transducer at $x = 0$ ($D < 0.2$). Therefore, it is reasonable to assume that the transducer is mostly sensitive to perturbations (e.g. corrosion) occurring in front of it and that the lateral dimensions of the sample (and thus wave reflections from the sides) will not affect its measurement.

5. Conclusions

A technique based on coda wave interferometry was proposed to quantify the thickness loss caused by saltwater corrosion on a steel sample. The method consists in measuring the coda stretching and the temperature as a function of time on the corroding sample, with respect to a reference chosen for the sample initial state. The stretching of the coda caused by temperature variations can easily be compensated on the corroding sample using either a control sample protected from corrosion or a relation between coda stretching and temperature. The temperature-corrected coda stretching factor is observed to correlate with an independent corrosion parameter computed from pictures of the onset of corrosion on the sample during a 60 h experiment in saltwater. A simple physical model of coda signals composed of longitudinal waves reflected off the sample opposite faces reveals that the coda stretching factor is proportional to the average corrosion depth. This relation was used to deduce the instantaneous average corrosion depth and corrosion rate during the experiment. The estimated average corrosion depth is validated by depth profiles measured after the experiment. As a result, the ultrasonic coda provides a precise real time local indicator of corrosion onset and development at the surface of a steel sample. This technique is potentially more precise than the other ultrasonic methods which are based on first arrival wave fronts that probe the thickness loss only once during their propagation. Future work include conducting chemical experiments with imposed corrosion rates to verify whether the method presented in this paper can quantitatively track the corrosion speed in real time. Additionally, the measurement setup will be deployed in situ to monitor corrosion of offshore and onshore metallic structures.

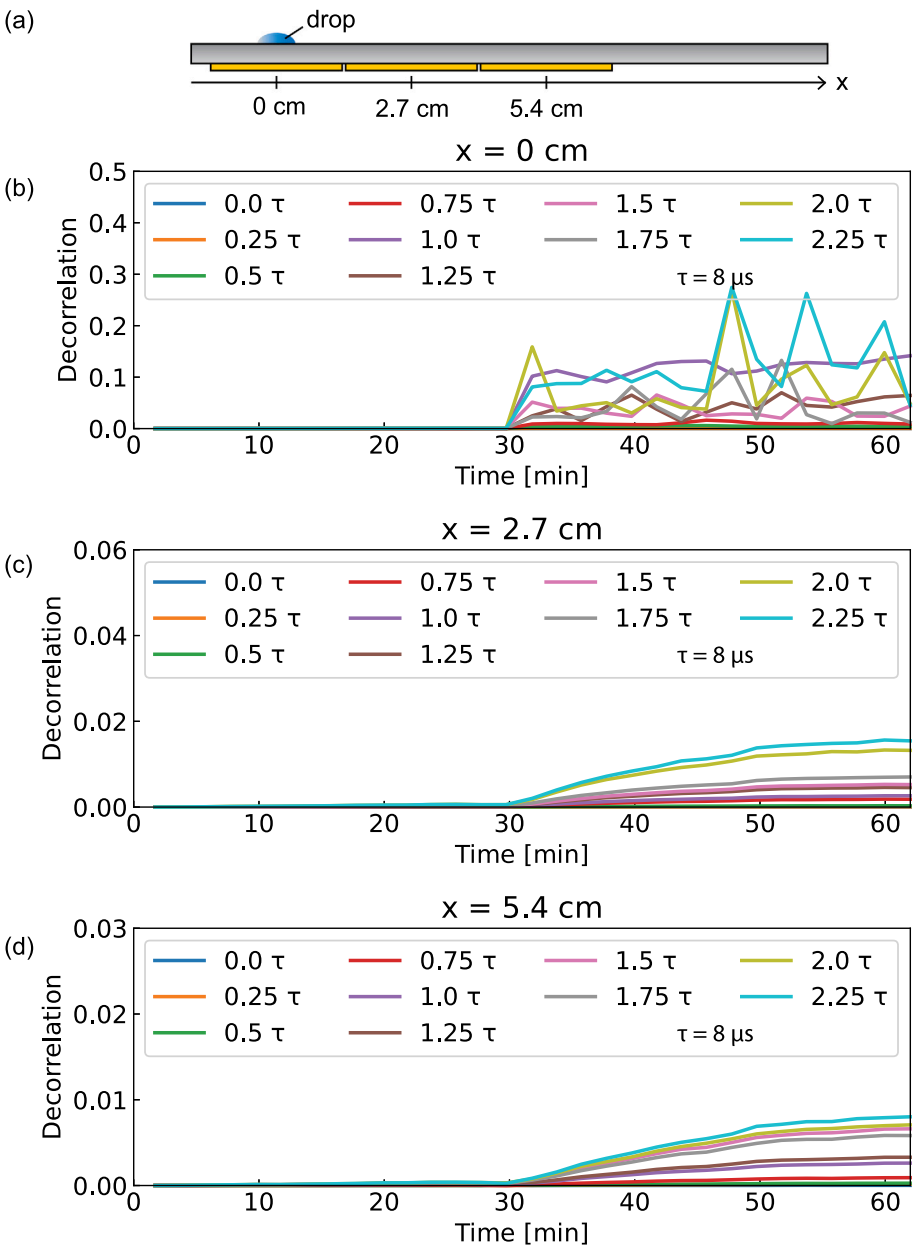

Fig. 12. (a) Schematic of the experiment with a 10-by-4 cm^2, 2 mm thick steel plate with three piezoelectric transducers side-by-side and a drop of water deposited in front on a transducer. (b), (c) and (d) Decorrelation curves recorded on the transducer at distances (b) $x = 0$ cm, (c) $x = 2.7$ cm and (d) $x = 5.4$ cm from the drop. The different colors represent different starting times of the 1 µs-long correlation window, normalized by the characteristic attenuation time $\tau \simeq 8$ µs.

CRediT authorship contribution statement

Maxime Farin: Conceptualization, Methodology, Software, Validation, Formal analysis, Investigation, Writing – original draft, Writing – review & editing, Visualization. **Emmanuel Moulin:** Conceptualization, Methodology, Resources, Supervision, Project administration, Funding acquisition, Writing – review & editing. **Lynda Chehami:** Conceptualization, Methodology, Resources, Supervision, Project administration, Funding acquisition, Writing – review & editing. **Farouk Benmeddour:** Conceptualization, Methodology, Resources, Supervision, Project administration, Funding acquisition, Writing – review & editing. **Cyril Nicard:** Conceptualization, Methodology, Investigation. **Pierre Campistron:** Conceptualization, Methodology, Resources, Supervision, Project administration, Funding acquisition, Writing – review & editing. **Olivier Bréhault:** Conceptualization, Methodology, Investigation. **Lucie Dupont:** Methodology, Resources.

Declaration of competing interest

The authors declare that they have no known competing financial interests or personal relationships that could have appeared to influence the work reported in this paper.

Acknowledgments

This work was supported by the European project Interreg 2 Seas, Antwerp Maritime Academy, SOCORRO. The authors thank Ingrid Proriol-Serre, David Balloy, Guillaume Delaplace and Simon Khelissa (Univ. Lille, CNRS, INRAE, Centrale Lille, UMR 8207 - UMET - Unité Matériaux et Transformations, F-59000 Lille, France) for helpful discussions.

References

[1] X. Qi, V. Gelling, A review of different sensors applied to corrosion detection and monitoring, Recent Pat. Corros. Sci. 1 (2011) 1–7, http://dx.doi.org/10.2174/2210683911101010001.

[2] R. Wright, P. Lu, J. Devkota, F. Lu, M. Ziomek-Moroz, P. Ohodnicki, Corrosion sensors for structural health monitoring of oil and natural gas infrastructure: A review, Sensors 19 (2019) 3964, http://dx.doi.org/10.3390/s19183964.

[3] T. Rommetveit, T. Johansen, J. Johnsen, A combined approach for high-resolution corrosion monitoring and temperature compensation using ultrasound, IEEE Trans. Instrum. Meas. 59 (2010) 2843–2853, http://dx.doi.org/10.1109/TIM.2010.2046598.

[4] F. Honarvar, F. Salehi, V. Safavi, A. Mokhtari, A. Sinclair, Ultrasonic monitoring of erosion/corrosion thinning rates in industrial piping systems, Ultrasonics 53 (2013) 1251–1258, http://dx.doi.org/10.1016/j.ultras.2013.03.007.

[5] F. Zou, F. Cegla, High accuracy ultrasonic monitoring of electrochemical processes, Electrochem. Commun. 82 (2017) 134–138, http://dx.doi.org/10.1016/j.elecom.2017.07.020.

[6] H. Liu, L. Zhang, H. Liu, S. Chen, S. Wang, Z. Wong, K. Yao, High-frequency ultrasonic methods for determining corrosion layer thickness of hollow metallic components, Ultrasonics 89 (2018) 166–172, http://dx.doi.org/10.1016/j.ultras.2018.05.006.

[7] M. Silva, R. Gouyon, F. Lepoutre, Hidden corrosion detection in aircraft aluminum structures using laser ultrasonics and wavelet transform signal analysis, Ultrasonics 41 (2003) 301–305, http://dx.doi.org/10.1016/S0041-624X(02)00455-9.

[8] H. Reis, B. Ervin, D. Kuchma, J. Bernhard, Estimation of corrosion damage in steel reinforced mortar using guided waves, J. Press. Vessel Technol. 38 (2005) 255–261, http://dx.doi.org/10.1115/1.1989352.

[9] B. Ervin, D. Kuchma, J. Bernhard, H. Reis, Monitoring corrosion of rebar embedded in mortar using high-frequency guided ultrasonic waves, J. Eng. Mech. 135 (2009) 9–19, http://dx.doi.org/10.1061/(ASCE)0733-9399(2009)135:1(9).

[10] P. Khalili, P. Cawley, The choice of ultrasonic inspection method for the detection of corrosion at inaccessible locations, NDT E Int. 99 (2018) 80–92, http://dx.doi.org/10.1016/j.ndteint.2018.06.003.

[11] X. Cao, L. Zeng, J. Lin, J. Hua, A correlation-based approach to corrosion detection with Lamb wave mode cutoff, J. Nondestruct. Eval. 38 (2019) 87, http://dx.doi.org/10.1007/s10921-019-0629-y.

[12] H. Mazille, R. Rothea, C. Tronel, An acoustic emission technique for monitoring pitting corrosion of austenitic stainless steels, Corros. Sci. 37 (1995) 1365–1375, http://dx.doi.org/10.1016/0010-938X(95)00036-J.

[13] C. Jirarungsatian, A. Prateepasen, Pitting and uniform corrosion source recognition using acoustic emission parameters, Corros. Sci. 52 (2010) 187–197, http://dx.doi.org/10.1016/j.corsci.2009.09.001.

[14] S. Hogg, B. Anderson, P.-Y. Le Bas, M. Remillieux, Nonlinear resonant ultrasound spectroscopy of stress corrosion cracking in stainless steel rods, NDT E Int. 102 (2019) 194–198, http://dx.doi.org/10.1016/j.ndteint.2018.12.007.

[15] R. Snieder, A. Grêt, H. Douma, J. Scales, Coda wave interferometry for estimating nonlinear behavior in seismic velocity, Science 295 (2002) 2253–2255, http://dx.doi.org/10.1126/science.1070015.

[16] A. Grêt, R. Snieder, J. Scales, Time-lapse monitoring of rock properties with coda wave interferometry, J. Geophys. Res. 111 (2006) B03305, http://dx.doi.org/10.1029/2004JB003354.

[17] Y. Zhang, O. Abraham, V. Tournat, A. Le Duff, B. Lascoup, A. Loukili, F. Grondin, O. Durand, Validation of a thermal bias control technique for coda wave interferometry (CWI), Ultrasonics 53 (2013) 658–664, http://dx.doi.org/10.1016/j.ultras.2012.08.003.

[18] T. Planès, E. Larose, A review of ultrasonic coda wave interferometry in concrete, Cem. Concr. Res. 53 (2013) 248–255, http://dx.doi.org/10.1016/j.cemconres.2013.07.009.

[19] B. Chen, D. Callens, P. Campistron, E. Moulin, P. Debreyne, G. Delaplace, Monitoring cleaning cycles of fouled ducts using ultrasonic coda wave interferometry (CWI), Ultrasonics 96 (2019) 253–260, http://dx.doi.org/10.1016/j.ultras.2018.12.011.

[20] B. Chen, M. Abdallah, P. Campistron, E. Moulin, D. Callens, S. Khelissa, P. Debreyne, N.-E. Chihib, G. Delaplace, Detection of biofilm formation by ultrasonic coda wave interferometry, J. Food Eng. 290 (2021) 110219, http://dx.doi.org/10.1016/j.jfoodeng.2020.110219.

[21] R. Weaver, O. Lobkis, Temperature dependence of diffuse field phase, Ultrasonics 38 (2000) 491–494, http://dx.doi.org/10.1016/S0041-624X(99)00047-5.

[22] Y. Lu, J. Michaels, A methodology for structural health monitoring with diffuse ultrasonic waves in the presence of temperature variations, Ultrasonics 43 (2005) 717–731, http://dx.doi.org/10.1016/j.ultras.2005.05.001.

[23] R. Melchers, R. Jeffrey, Early corrosion of mild steel in seawater, Corros. Sci. 47 (2005) 1678–1693, http://dx.doi.org/10.1016/j.corsci.2004.08.006.